BUREAU OF RECLAMATION

# Rotor Installed Corona Mapping of Stator Windings within Large Diameter Hydro Generators

**Science and Technology Program**
**Research and Development Office**
**Final Report No. ST-2021-19078-01**


**U.S. Department of the Interior**

September 2021

# REPORT DOCUMENTATION PAGE

*Form Approved*
*OMB No. 0704-0188*



| 1. REPORT DATE *(DD-MM-YYYY)* | 2. REPORT TYPE | 3. DATES COVERED *(From - To)* |
|---|---|---|
| 30-09-2021 | Research | October 1, 2019 – September 30, 2021 |

**4. TITLE AND SUBTITLE**
Rotor Installed Corona Mapping of Stator Windings within Large Diameter Hydro Generators

**5a. CONTRACT NUMBER**
RR4888FARD1903001/F021A

**5b. GRANT NUMBER**

**5c. PROGRAM ELEMENT NUMBER**
1541 (S&T)

**6. AUTHOR(S)**
Jacob Lapenna, Electrical Engineer

**5d. PROJECT NUMBER**
Final Report ST-2021-19078-01

**5e. TASK NUMBER**

**5f. WORK UNIT NUMBER**

**7. PERFORMING ORGANIZATION NAME(S) AND ADDRESS(ES)**
Technical Service Center
Hydropower Diagnostics and SCADA Group
Bureau of Reclamation
Denver Federal Center
P.O. Box 25007
Denver, CO 80225

**8. PERFORMING ORGANIZATION REPORT NUMBER**

**9. SPONSORING/MONITORING AGENCY NAME(S) AND ADDRESS(ES)**
Science and Technology Program
Research and Development Office
Bureau of Reclamation
U.S. Department of the Interior
Denver Federal Center
PO Box 25007, Denver, CO 80225-0007

**10. SPONSOR/MONITOR'S ACRONYM(S)**
Reclamation

**11. SPONSOR/MONITOR'S REPORT NUMBER(S)**
Final Report ST-2021-19078-01

**12. DISTRIBUTION/AVAILABILITY STATEMENT**
Final Report may be downloaded from https://www.usbr.gov/research/projects/index.html

**13. SUPPLEMENTARY NOTES**

**14. ABSTRACT**
This research utilized near field communication antennas to map partial discharge activity, with slot level resolution, throughout a stator winding of a service aged hydro generator with minimal disassembly of the asset and without the need to remove the rotor. Results suggest that, with further research and development, this method may be a viable replacement for conventional corona probe testing. As a replacement, this method would allow for trending of partial discharge activity in each slot of large stator windings while significantly reducing costs, hazards, and risks associated with obtaining this data, which would be a substantial leap in diagnostic capabilities within the industry.

**15. SUBJECT TERMS**
Partial Discharge, Corona Probe, Condition Based Maintenance, Near Field Communication, Asset Management

| 16. SECURITY CLASSIFICATION OF: | | | 17. LIMITATION OF ABSTRACT | 18. NUMBER OF PAGES | 19a. NAME OF RESPONSIBLE PERSON |
|---|---|---|---|---|---|
| a. REPORT | b. ABSTRACT | THIS PAGE | | | Jacob Lapenna |
| U | U | U | | 36 | 19b. TELEPHONE NUMBER *(Include area code)* (303) 445-2829 |

# Mission Statements

The Department of the Interior (DOI) conserves and manages the Nation's natural resources and cultural heritage for the benefit and enjoyment of the American people, provides scientific and other information about natural resources and natural hazards to address societal challenges and create opportunities for the American people, and honors the Nation's trust responsibilities or special commitments to American Indians, Alaska Natives, and affiliated island communities to help them prosper.

The mission of the Bureau of Reclamation is to manage, develop, and protect water and related resources in an environmentally and economically sound manner in the interest of the American public.

# Disclaimer

Information in this report may not be used for advertising or promotional purposes. The data and findings should not be construed as an endorsement of any product or firm by the Bureau of Reclamation, Department of Interior, or Federal Government. The products evaluated in the report were evaluated for purposes specific to the Bureau of Reclamation mission. Reclamation gives no warranties or guarantees, expressed or implied, for the products evaluated in this report, including merchantability or fitness for a particular purpose.

# Acknowledgements

The Science and Technology Program, Bureau of Reclamation, sponsored this research.

# Rotor Installed Corona Mapping of Stator Windings within Large Diameter Hydro Generators

**Final Report No. ST-2021-19078-01**

*prepared by*

**Technical Service Center**
**Jacob Lapenna, Electrical Engineer**

# Peer Review

## Bureau of Reclamation
## Research and Development Office
## Science and Technology Program

Final Report ST-2021-19078-01

**Rotor Installed Corona Mapping of Stator Windings within Large Diameter Hydro Generators**

JACOB LAPENNA
Digitally signed by JACOB LAPENNA
Date: 2021.09.10 10:57:09 -06'00'

**Prepared by: Jacob Lapenna**
**Electrical Engineer, Technical Service Center, Hydropower Diagnostics and SCADA Group**

ERIC EASTMENT
Digitally signed by ERIC EASTMENT
Date: 2021.09.13 08:36:05 -06'00'

**Peer Review by: Eric Eastment, PE**
**Electrical Engineer, Technical Service Center, Hydropower Diagnostics and SCADA Group**

NATHAN MYERS
Digitally signed by NATHAN MYERS
Date: 2021.09.13 10:03:03 -06'00'

**Verified by: Nathan Myers, PE**
**Manager, Technical Service Center, Hydropower Diagnostics and SCADA Group**

*"This information is distributed solely for the purpose of pre-dissemination peer review under applicable information quality guidelines. It has not been formally disseminated by the Bureau of Reclamation. It does not represent and should not be construed to represent Reclamation's determination or policy."*

# Acronyms and Abbreviations

| | |
|---|---|
| AC | Alternating Current |
| API | Application Programming Interface |
| COM | Component Object Model |
| CW | Clockwise |
| CCW | Counterclockwise |
| DC | Direct Current |
| EMRT | Electromagnetic Rotor Turner |
| IEC | International Electrotechnical Commission |
| NFC | Near Field Communication |
| OPR | Once Per Revolution |
| PD | Partial Discharge |
| PDF | Probability Density Function |
| Reclamation | Bureau of Reclamation |
| RISE | Reclamation Information Sharing Environment |
| USB | Universal Serial Bus |

# Measurements

| | |
|---|---|
| GHz | gigahertz |
| Hz | Hertz |
| kHz | kilohertz |
| kV | kilovolt |
| MHz | megahertz |
| m | meter |
| MVA | megavolt Ampere |
| µs | microsecond |
| ms | millisecond |
| nC | nanocoulomb |
| nF | nano-farad |
| Ω | Ohm |
| s | second |
| V | Volt |

# Contents

Page

# Executive Summary

Stator winding insulation failures in large rotating machines can often be unpredictable and cause long unscheduled outages and costly repairs. One good indicator for trending insulation health throughout an asset's life is via partial discharge (PD) activity. This is because PD activity is a direct result of defective or degraded insulation and can compound on itself degrading the insulation even further. As such, online PD monitoring has been widely adopted throughout the industry. This technology typically relies on galvanically decoupling PD signals from the power voltage at specific locations within the machine. For large diameter machines, this decoupling cannot sense signal very far from the decoupling location, leaving the monitoring system blind to a large portion of the machine. Other remote sensing technologies exist, though are also limited in the number of stator coils that can be measured. Only corona probe testing can obtain a full picture of the entire winding. However, due to the significant disassembly and hazards involved with corona probe measurements, this test is rarely performed.

This research sought to advance previous feasibility studies which determined near-field communication (NFC) antennas could be utilized to remotely sense PD activity within service aged stator windings. The work discussed here expanded on this concept and adapted commercially available PD monitoring equipment to measure PD from an NFC antenna. Using electromagnetic means to slowly turn a rotor with an NFC antenna mounted to a pole face, PD activity throughout a 330-slot stator winding was mapped to the source slot numbers. Unlike traditional corona probe, the only disassembly required for this testing was the removal of one deck plate and one air baffle.

This report mainly focuses on the prototypical PD mapping system. The data collected and discussed in this report, the software written to analyze this data, and the software written to operate the prototypical PD mapping system can all be found on the Reclamation Information Sharing Environment (RISE)[1]. The following list covers the deliverables discussed in detail here and obtainable on RISE:

- This report
- OmiCOMServer
    - A program written in C# for initializing and streaming data from the Omicron MPD system.
- OmiCOMClientCPP
    - A program written in C++ for consuming and recording the data served by the OmiCOMServer program.
- Analyzer
    - A Python application programming interface (API) for more easily and efficiently interacting with the recorded data and creating meaningful visuals, along with a README.txt file briefly documenting the use of this API.
- Data

[1] https://data.usbr.gov/

    - The plaintext, comma separated data recorded by the prototype PD mapping system along with a README.txt file detailing testing notes and configurations relevant to the data files.
- Streams
    - Omicron stream files of PD from a service aged stator bar, measured in the laboratory, using an NFC antenna, traditional corona probe, and Omicron 2 nF capacitive coupler for comparison. These stream files are also accompanied by a README.txt file detailing test setups and conditions.

The above deliverables are made available to aid in collaboration with outside entities. This study clearly shows that it is possible to map PD activity throughout a service-aged stator winding with minor adaptations to a commercially available PD monitoring system. Such capabilities could have wide- and far-reaching implications for asset management in the future if a commercial system utilizing this technology was made available. Sparking such advancements in the industry is the ultimate goal of this work.

# Introduction

## Background

The present diagnostics landscape for in-situ, non-invasive testing of high-voltage insulation systems in large rotating machines is limited. Because insulation system failures are a major cause of end-of-life events in these assets, there remains a lot to be gained in efficiency and productivity by even minor improvements in diagnostic testing. The predominantly accepted test suite for non-invasive diagnostics is mostly limited to determining average insulation condition over the entire insulation system rather than localized defects or even specific issues. It has been shown in past research that even modern forms of cost-effective online monitoring of partial discharge (PD) is limited and can only detect issues from a small portion of an entire asset's insulation system (Lapenna and Eastment, Power System Diagnostics).

This determination of average insulation condition is formed from extensive knowledge after searching for correlations across different measurements and across the same measurements over time. Such assessments also rely on significant analysis of operating and maintenance history to support these determinations of asset condition. Even after this extensive testing and analysis, results are often indistinct and reported conditions based on likelihoods and probable causes. Reporting an asset's likely condition leaves the asset manager with increased uncertainty in management decisions and perpetuates the need for interval-based maintenance rather than condition-based maintenance.

Mapping PD throughout the stator winding via corona probe testing has long been viewed as one of the best tests for determining actual insulation condition with a higher level of certainty. However, traditional corona probe testing techniques require rotor removal and are associated with significant outage time, risks, safety hazards, and overall cost. Due to the complexity involved in performing a traditional corona probe test, this important diagnostic data is rarely obtained if it is collected at all. A widely accessible method to perform this high-value test without the associated high-cost, risks, and safety hazards could represent a considerable leap in diagnostic capabilities across the industry.

If mapping of PD became a routine test, it would open the door to many more options for managing an asset. Specific issues could be trended over time to help forecast end-of-life timelines more reliably. By examining the stator winding health on a slot-by-slot basis, this diagnostic method may provide the asset manager the opportunity to perform life extension repairs. Issues could be localized, supporting decisions on whether they require relatively minor repair or an entire rewind or, if possible, even a configuration change like line-neutral interchange. Based on the data, it may be possible to selectively replace stator coils, or bars, that have approached end-of-life faster than others. Over time, with sufficient data across asset fleets, common issues may be better identified, and better insulation systems engineered and manufactured in the future. By more accurately determining insulation condition, more general bulk testing could be put off until the condition of the asset warrants further testing and maintenance, more closely aligning with condition-based maintenance practices.

## Previous Work

Extensive work has been carried out in developing a means of low-cost, reliable PD mapping without the need to remove an asset's rotor. The first project was funded in 2017. This project, titled "Feasibility of Rotor Installed Machine Corona Mapping with Patch Antennas", was assigned project number 1711. The second project was funded in 2019 and is ongoing. This most recent project is titled "Rotor Installed Corona Mapping of Stator Windings within Large Diameter Hydro Generators" and was assigned project number 19078. This project and its associated funding is scheduled to close out at the end of this fiscal year.

Previous research investigated the feasibility of using thin, flexible patch antennas to detect PD (Lapenna, Feasibility of Corona Mapping Using Patch Antennas). Various commercially available patch antennas were investigated in a laboratory environment which simulated the antennas being mounted on a pole face with PD emanating from within a service-aged stator coil across a one-inch air gap from the antenna. For a variety of technical reasons described in this project's closeout report, it was determined that near-field communication (NFC) antennas were best suited for detecting PD when compared to capacitive style patch antennas. NFC antennas are commonly found in touchless card readers and smart phones and allow for such functionality as contactless payment on smart phones when the phone is held near (though not touching) a point-of-sale device. Due to the prevalence of NFC antennas in consumer electronics, they can easily be sourced from many suppliers, often for less than a dollar per antenna.

Once feasibility was demonstrated, funding was sought to further test these NFC antennas in the field and develop a prototypical system to demonstrate corona mapping of a real machine within Reclamation's fleet. Funding was granted, and this was the focus of this research project. The first field test was carried out by mounting an NFC antenna on an articulating head at the end of an electrically insulated pole, or 'hot stick', and performing PD mapping on a machine at rated phase-to-ground voltage with the rotor removed. The articulating head allowed the antenna to maintain a set distance from, and surface angle to, the stator's surface, which simulated the antenna's distance and angle if it were mounted on a rotor pole face. Like traditional corona probe testing, these tests were carried out with the articulating head by manually placing the antenna near the surface of each slot and recording the voltage induced in a voltmeter connected to the antenna. The voltmeter used was that of the traditional corona probe test set. This testing was performed side-by-side with traditional corona probe testing for comparison.

Once detection of PD within a real stator winding was verified to be possible using the NFC articulating probe, a more advanced prototype was constructed to show proof of concept for rotor in PD mapping of stator windings. This prototype and the subsequent data collected was the main goal of this research and is the bulk of the discussion in this report.

## Objectives

The goal of this research project was to obtain field test results which show that PD activity could be mapped to its corresponding slot or coil group within a service aged stator winding without the need to remove the rotor or exposed personnel or equipment to undue hazards and risks. This goal was reached in stages over the three-year funding window allotted for this project. Using the NFC

antennas previously studied in past research, the steps to reach the overall goal, each of which are discussed in more detail in the sections below, are listed as follows:

1. Investigate amplification of the analog signal from the NFC antenna when measuring PD in the laboratory.
2. Use signal amplification methods determined in the previous step to build an NFC probe to be used analogous to a traditional corona probe.
3. Use the NFC probe constructed in the previous step to perform field testing on a service aged stator winding with the rotor removed.
4. Once field testing was shown to be feasible, construct a prototypical system by adapting more advanced commercially available PD measurement equipment to detect PD from the NFC antenna.
5. Using the prototype from the previous step, perform PD mapping of a service-aged stator winding, in the field, with the rotor installed and without personnel inside during the test.
6. Using the data acquired in the previous step, create an application programming interface (API) to analyze and visualize test results with the intent of easing future advancement of the prototype.

# Methods

## Analog Signal Amplification

During the initial feasibility studies, it was determined that the NFC antenna's analog signal, as measured by a high-impedance measurement device such as an oscilloscope, was several orders of magnitude lower than a traditional PD coupler measured on the same device. For this reason, methods of amplifying the analog signal from the NFC antenna were investigated. The Texas Instruments® THS4303 wideband fixed-gain amplifier was selected for this purpose due to its large bandwidth (1.8 GHz), high slew rate (5,500 V/μs), and low distortion (Texas Instruments, THS4303 Datasheet). For ease of incorporation into the NFC antenna probe, the THS4303EVM evaluation board containing this amplifier was used, which was already impedance matched for 50 Ω terminations and soldered with power input terminals on board. Figure 1 shows this evaluation board along with its ideal frequency response for small input signals (Texas Instruments, THS4303 Datasheet). The frequency response shows nearly constant gain from very low frequencies to around 100 MHz. Because NFC antennas are designed with a center frequency of 13.5 MHz, this amplifier easily covers the antenna's frequency band. Moreover, due to the very wide band of the amplifier, signals of interest away from the antenna's center frequency should also be amplified proportionally, which is advantageous when the exact band of the PD's target signal is not known.

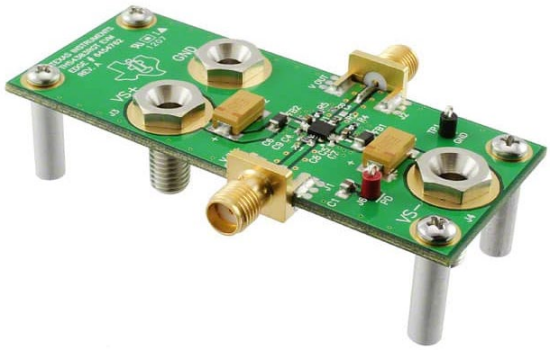

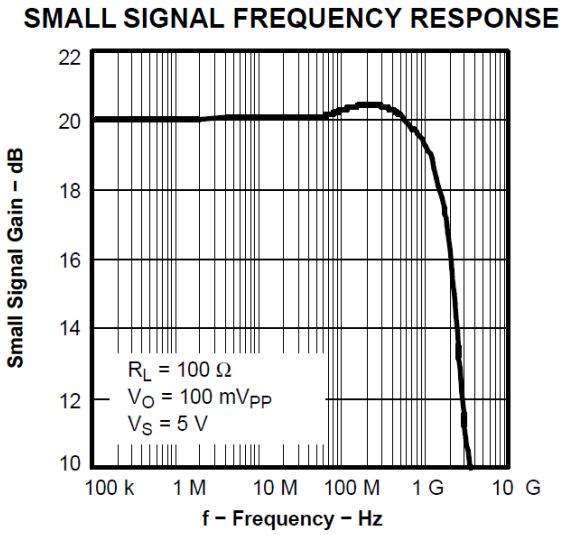


(a) (b)

Figure 1 THS4303EVM board (a) and its gain frequency response (b).

To incorporate the amplifier board into the overall NFC antenna probe, a printed circuit was designed, and its construction outsourced. This circuit board incorporated two direct current (DC) 9 V batteries, a DC-to-DC voltage converter, provisions for mounting the amplifier board, and printed traces for appropriately connecting all these components together. The DC-to-DC voltage converter allowed conversion of the fluctuating 9 V battery voltage (battery voltage decreases as its initial charge is consumed) to a constant ±5 V source for the active amplifier. The antenna was connected to the amplifier and the amplifier output to the measurement device via coaxial cable. All this componentry was then mounted on a hot stick with an articulating head making up the NFC antenna probe.

## NFC Antenna Probe

Like the traditional corona probe, the NFC antenna probe would have to be placed and held by personnel on the surface of an energized stator winding's slots. Due to the probe's proximity to potentially large static surface charges (e.g. the end windings) during testing, the entire probe had to be electrically isolated from the test operator. It is not the intention for the corona probe, nor the NFC antenna probe, to contact the stator end windings. This would be hazardous to the operator. For the NFC probe, operator isolation was achieved by powering all active components with batteries and mounting the whole probe at the end of a hot stick. In this way, the test operator could place the probe at a desired measurement location on the stator with minimal risk of electric shock. To further mitigate risk, the person handling the hot stick wore high voltage insulated gloves, and the person taking measurements did not touch the measurement meter while the probe was in position for a measurement.

The NFC antenna was mounted to an articulating head to ensure the inductive field was orthonormal to the surface of the antenna and measurement point regardless of the angle at which the operator applied the probe via the hot stick. Spacers were also added to this articulating head to ensure the antenna maintained a distance of 1 inch from the measurement surface. This spacing

simulated the antenna being mounted on a rotor pole face with a 1-inch air gap between the rotor and stator. To simulate the antenna being mounted on pole iron, and prevent stray eddy currents from attenuating induced signal, EM15TF-012-1 3M® Flux Field Directional Material was used as a backing for the antenna on the face of the articulating head. Figure 2 shows a picture of the NFC antenna probe connected to the corona probe voltage meter on a telescoping hot stick (bottom). The face of the articulating head with the NFC antenna and iron backing is shown in the upper left inset. The amplifier board, mounted to the custom printed board, with batteries is shown in the upper right, with the jumper wire for keeping the amplifier in its power-save mode until the probe is in use.

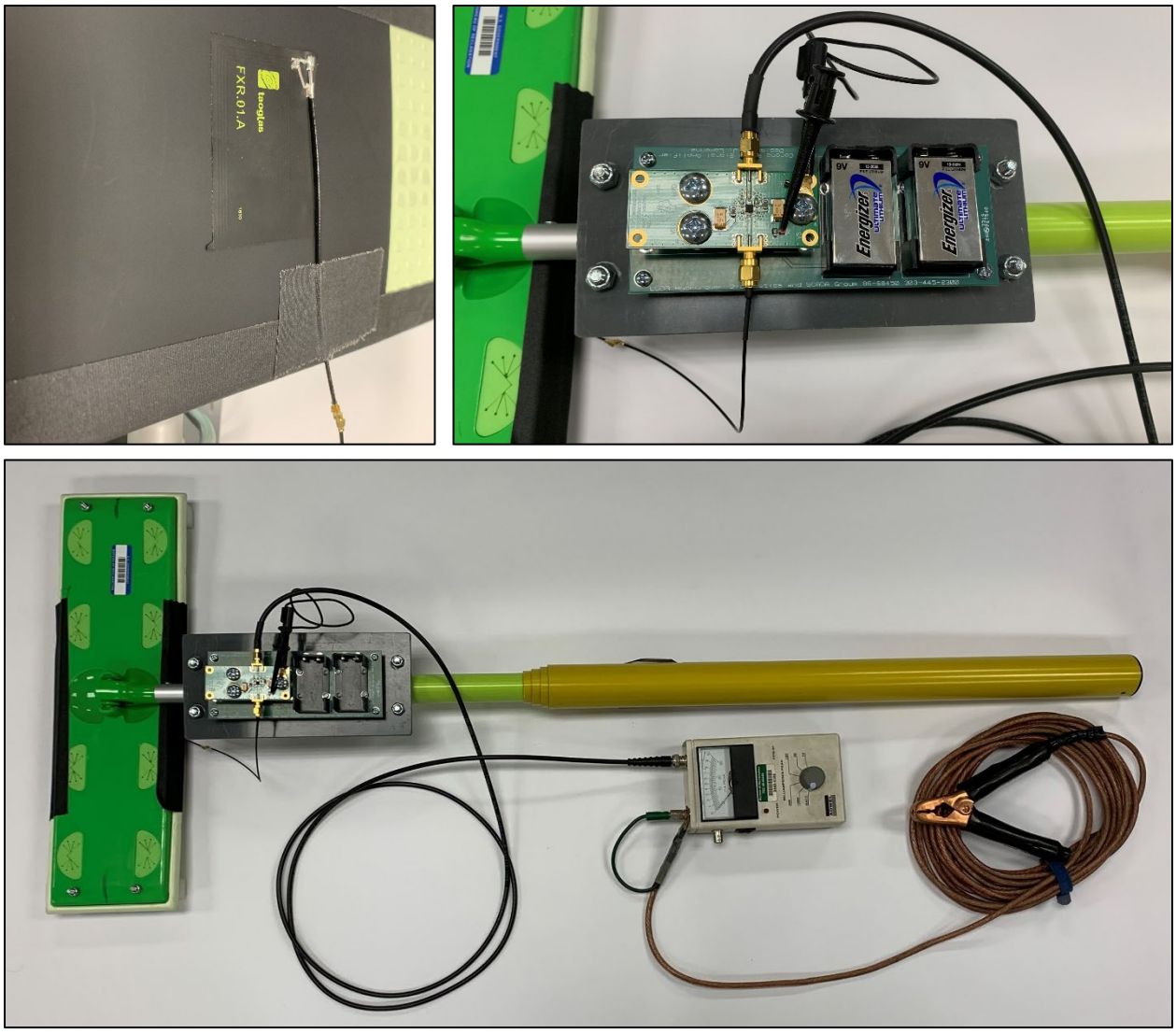


Figure 2 Photo of the NFC antenna probe with corona probe meter and amplifier.

The amplified signal was then connected to the voltmeter of an Iris Power® PPM-97 corona probe test set. This meter, referred to as a peak-pulse meter, has an analog meter which shows the peak voltage induced in the connected probe within the meters input pass band. For the connected probe held at a given measurement location, large voltages above the noise threshold correlate to more intense PD activity and lower voltages above the noise threshold correlate to less intense PD

activity. Because the meter's pass band may not align with the NFC pass band, this behavior was verified with the NFC antenna in the laboratory using service-aged stator coils energized at their rated line-to-ground voltages. Coils with higher known levels of PD activity increased analog meter readings when connected to the amplified NFC antenna and coils with lower known levels of PD activity showed decreased analog meter readings. In addition, a transmitting NFC antenna was connected to PD calibration equipment and placed within proximity and facing the receiving NFC antenna of the makeshift probe. Larger voltages were also seen on the analog meter when larger PD pulses from the calibrator were input into the transmitting NFC antenna. Analog meter readings also decreased as the NFC antenna probe's distance from the source increased.

## NFC Probe Field Testing

Tests utilizing the NFC antenna probe were carried out on Grand Coulee Generator No. 22 (G-22) in September 2019. The nameplate rating of G-22 is 825.69 MVA at 15 kV. The outer diameter of the stator approaches 23 m, with a stator core stack height of 2.1 m. There are 540 slots in the stator winding. The rotor was removed for mechanical refurbishment and testing was conducted during a routine condition assessment of the asset's electrical components. This condition assessment testing was conducted during a narrow window within the overall outage and only one test with the NFC antenna probe could be carried out.

The NFC antenna probe testing was performed with all three phases of the stator winding simultaneously energized to 8.66 kV line-to-ground voltage using a series resonant alternating current (AC) high-potential test set. The NFC antenna probe was then placed over all 540 slots of the stator winding near the middle of the axial length of each slot. The narrow test window did not allow sufficient time for the probe to be run along the axial length of each slot to find the highest reading in each slot as would normally occur during a traditional corona probe test.

Traditional corona probe testing was also performed as part of the condition assessment testing. Because this testing was part of the asset condition assessment, more priority, and therefore more time within the narrow testing window, was allocated for this test. This test was performed on each phase individually, with only one phase energized at a time, and only the slots with a top bar corresponding to the energized phase measured. For each phase's test, the other phases not under test were grounded. This setup provided voltage stress to the ground wall insulation, grading treatment, and phase-to-phase insulation, whereas the NFC antenna probe test setup only provided voltage stress to the ground wall and grading treatment. Moreover, for every slot measured with the corona probe, the corona probe was run along the axial length of the slot, and the highest reading was taken as the relative PD intensity for that slot.

The test results of both probes can be seen in Figure 3. Specifically, each plot shows the traditional corona probe measurements along with the single NFC antenna probe's measurements repeated in each plot for comparison. The discontinuity in the corona probe data is due to only measuring the energized slots for the respective test run. Due to the difference in test setup between the NFC antenna probe and corona probe measurements, any quantitative correlation between the two results was not sought. The goal of the testing was to simply determine whether PD activity could be detected with slot (or coil-group) resolution using an NFC antenna. It is expected that different amplification, impedance matching, and test procedures between the two probes produces differing

outputs. However, like the corona probe data, the NFC antenna probe data does have plot features that span single slots and coil groups. This is evident as the slots spanning each coil group is highlighted for each phase in that phase's respective test plot. The various peaks and spikes of the NFC antenna probe data fit within many of these highlighted coil groups. This result was sufficient to proceed in building a more advanced PD mapping prototype as discussed in the next sections.

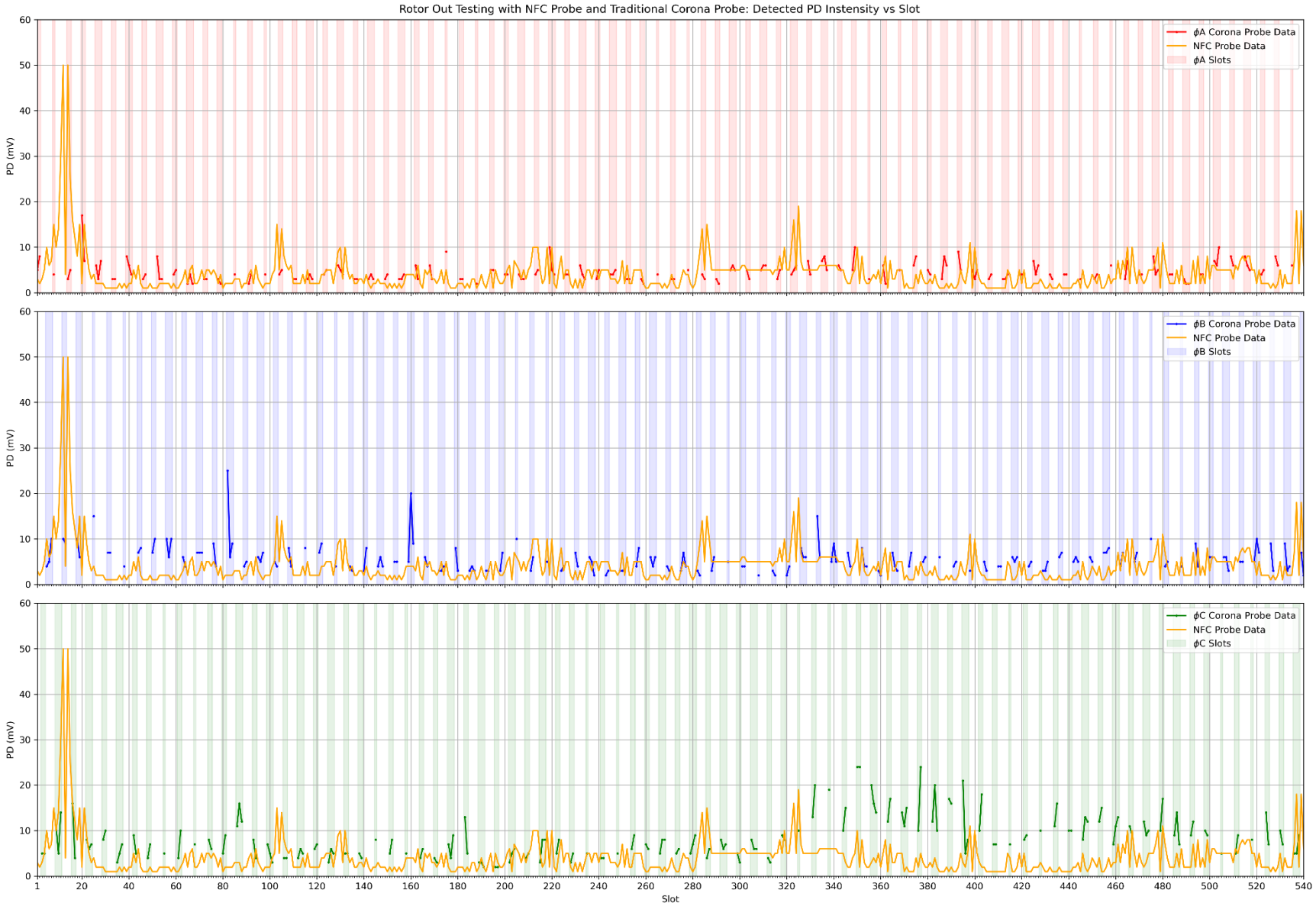


Figure 3 PD intensity versus slot as measured from NFC probe and corona probe.

## Prototypical System

To measure PD events from an NFC antenna, an Omicron® MPD 600 with an MCU 502 was used. The Omicron system was selected for this research due to its selective measurement bands and its use of the component object model (COM) within its software binary (discussed in more detail later).

As determined in the laboratory using a segment of a service-aged stator bar, direct connection of the NFC antenna to the PD channel of the MPD 600 produced reliable phase resolved PD patterns. Because the MPD 600 system is a wide band device, and the measurement band can be selected with the accompanying software, an amplifier was not needed for the NFC antenna's signal. Figure 4 shows these measurement results. The coil segment measured was removed from a service-aged stator winding at Flat Iron Powerplant. The segment has known issues with delamination and severe degradation of the insulation components within the epoxy and mica insulation system.

Figure 4 (a) and (c) show PD activity detected by the NFC antenna positioned with a 1-inch air gap between the specimen and antenna. Figure 4 (b) and (d) show PD activity detected with an Omicron 2 nF capacitive coupler galvanically connected to the specimen. The data from both the antenna and coupler were collected at the same time with multiple MPD 600 devices connected to the same MCU 502. The specimen was placed inside a grounded slot composed of iron laminations and energized with an 8 kV, 60 Hz sine wave. The selectable measurement band for both data channels was set to 1.5 MHz centered at 13.5 MHz, which is the center frequency for which NFC antennas are designed. The Omicron stream files for these tests, along with a README.txt file detailing the test setup for each stream file, can be found on the Reclamation Information Sharing Environment (RISE) site[2].

[2] https://data.usbr.gov/

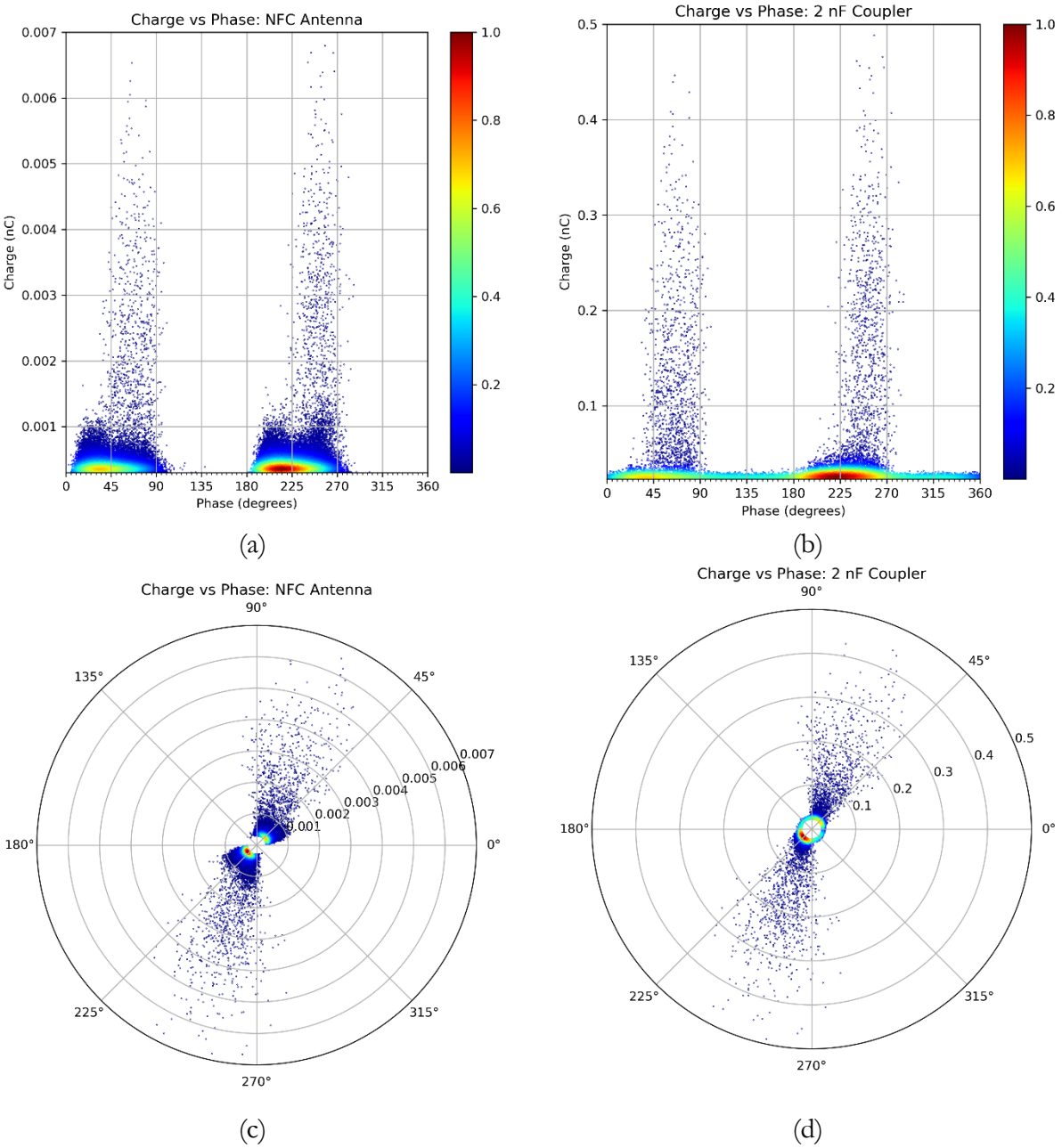


Figure 4 Phase resolved PD, from NFC antenna and 2 nF coupler, for a service aged stator bar segment.

Figure 4 shows color mapping related to a normalized probability density function (PDF) for each channel's PD. This is a function which estimates the probability of obtaining a PD sample of a given magnitude at a given phase. The normalization means a PD event corresponding to 1.0 on the color scale has the highest probability of being measured during any 60 Hz power cycle relative to all other PD events encountered. This PDF directly correlates to pulse frequency. In other words, PD events with higher probability of occurrence will be detected more frequently than events with low probability.

Note that the measurement band for the data shown in Figure 4 is tuned for optimal detection via the NFC antenna. This measurement band is likely sub-optimal for the capacitive coupler, as this coupler is designed for measurements conforming to the International Electrotechnical Commission (IEC) 60270 standard's frequency band of 300 kHz and centered at 250 kHz (IEC 60270:2000). Figure 5 (b) and (d) show detected PD from the 2 nF coupler when tuned to this IEC conforming band. Because the IEC band is two orders of magnitude lower than the NFC band, only noise was present on the NFC antenna for this measurement (Figure 5 (a) and (c)). The test specimen was a short section of stator bar (rather than a full bar) without grading treatment, significant surface discharges can therefore be seen on a portion of the negative half cycle (approximately 225 to 270 degrees) which is not present on this coupler in the 13.5 MHz centered band. This suggests that the capacitive coupler has more versatility and can detect the same high-frequency events that the NFC antenna detected at 13.5 MHz, while also being able to detect lower-frequency surface discharges that the NFC antenna cannot. More investigation will be needed in the future to determine whether the NFC antenna can produce meaningful phase resolved patterns which correlate to specific insulation conditions as the capacitive coupler can.

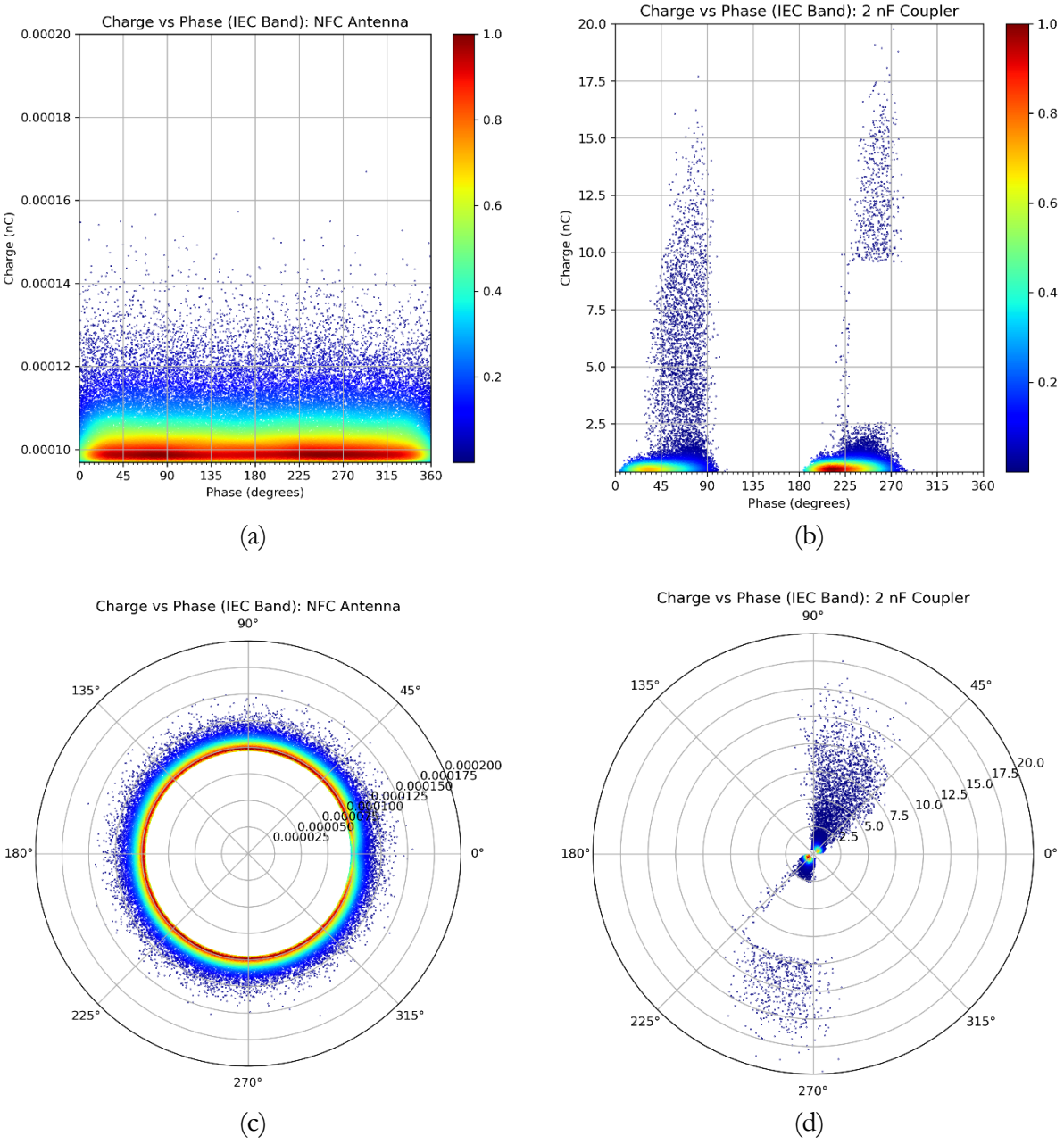


Figure 5 Phase resolved PD, from NFC antenna and 2 nF coupler, with 300 kHz band centered at 250 kHz.

The lack of measurement bandwidth associated with the NFC antenna is a necessary tradeoff for its remote sensing capabilities. While the NFC antenna cannot detect lower frequency PD events, its remote sensing capabilities gives it the potential to map PD throughout a stator winding with slot level resolution, which a galvanically connected capacitive coupler cannot achieve.

Decoupling PD event signals from the stator voltage at one or more locations galvanically is limited in that it can only detect PD events originating relatively close to the decoupling location. The overwhelming majority of the insulation system in a large diameter rotating machine cannot be

monitored with a typical decoupling scheme. To gain resolution within and throughout the stator winding, remote sensing of the fields generated by PD events must be carried out. Remote sensing of these fields is the only means of in-situ non-destructive mapping of PD activity over an entire winding with slot-level resolution. The idea is simple, if an antenna (or antennas) capable of sensing these fields can be placed throughout the unit, with the measured PD activity recorded relative to the position it was measured at, then precise mapping of this PD activity can occur. With traditional corona probe (and the NFC antenna probe), the antenna was located by a test operator that had to enter the stator bore (requiring rotor removal) and record individual measurements at individual locations. This manual process is cumbersome, time consuming, hazardous, and expensive.

At least one commercially available product can circumvent some manual testing by permanently installing antennas within every slot of interest (Iris Power, Stator Slot Couplers). This system performs remote sensing and offers slot-level resolution, though an antenna needs to be installed in every slot to be monitored. The number of antennas (and therefore data throughput) increases with the number of slots monitored. Even only monitoring slots with bars at 75% nameplate voltage or higher would require many antennas to be installed in a large-diameter machine with several parallel circuits per phase. It is unknown whether such a system can handle the data throughput such a large collection of antennas would generate. If, instead, a single antenna (or single antenna array) could be installed on a rotor pole and made to sense PD activity while the rotor turns, then PD activity could be mapped throughout the entire stator winding. This was the focus of this research—adapt the MPD 600 measurement system to work with an NFC antenna mounted on a rotor pole to map PD throughout a stator winding. To do this, the rotor must be turned in a controlled manner.

The Hydropower Diagnostics and SCADA Group within Reclamation's Technical Service Center (TSC) has developed the capability to turn rotors slowly and precisely, in-situ, via remote electrical means, across most of Reclamation's fleet (Lapenna, Development of Rotor Turning Device). The internally developed apparatus for achieving this purpose is known as the Electromagnetic Rotor Turner (EMRT). To turn a rotor, the EMRT utilizes timed switching of DC current within one phase of the stator winding, and constant DC current within the field winding, to turn the machine as a relatively low powered DC motor. By modulating the switching appropriately, arbitrary turning and positioning of the rotor is achievable. The EMRT is frequently used for routine testing such as obtaining air gap measurements across the entire circumference of an asset and calculating circularity, concentricity, and stator and rotor shape from these measurements. With the ease of slowly and precisely turning rotors with the EMRT, placing an NFC antenna on the rotor, and turning it to measure PD from each slot of the stator winding was a natural extension of the equipment's use.

Two data sources are required for rotor turning PD mapping to be performed: the signal from the NFC antenna from which PD events can be extracted, and data which can be used to precisely determine which slot the NFC antenna is in front of for each PD event measured. As shown, PD events can readily be acquired from the NFC antenna when connected to the PD channel of the MPD 600. For tracking the antenna's position, a capacitive proximity sensor was used. Specifically, a Baker Hughes® 400202 20 mm air gap probe was used to determine rotor position with slot-level accuracy. This air gap probe works by sensing capacitance with respect to ground. When in front of a grounded surface, the sensor's driver transduces the capacitance between the probe and the grounded surface to a proportional voltage with a linear range between 1 and 10 VDC (Baker Hughes, 4000 Series Air Gap Sensor). Because capacitance is a function of distance, as the distance changes, the capacitance (and therefore transduced voltage) also changes. The voltage from the air

gap sensor system is therefore directly proportional to the distance between the sensor and the grounded surface directly in front of it.

When an air gap probe is mounted on a rotor pole face and the rotor is turned, the recorded voltage signal over one revolution of a 330-slot machine appears as shown in Figure 6. The overall bulk variance of the signal over the entire revolution is due to irregularities in the air gap of the machine (some points on the stator are closer to the rotor than others). However, of substantial importance to the purposes of this project are the local maxima and minima in the upper-left inset showing the central zoomed portion of the plot. These local extrema are due to the stator bars being set back within their slots relative to the core teeth, meaning the distance between the sensor face and stator bar copper is larger than the distance between the sensor face and an iron core tooth. This means that the local maxima correspond with slot locations, and the local minima correspond with stator core teeth. By writing an algorithm which counts local maxima from a known starting location, exact slot position of the air gap sensor (and thereby the NFC antenna) can be determined.

For this reason, it is important to reference each rotation to a specific point to count maxima from. This is done with a once-per-revolution (OPR) signal. Specifically, the OPR signal is a signal encountered once, at a specific location, every revolution. For the prototype, this was done by taping a piece of grounded copper wire to a stator core tooth. The wire protruded out into the air gap and contacted the air gap sensor's face every revolution, driving the air gap sensor voltage to a very low value. The OPR signal is the large downward spike in the right inset of the image showing the zoomed portion at the end of the revolution. This data set was obtained by simply connecting the air gap sensor voltage into the V channel of the MPD 600 device and collecting the data with custom written software.

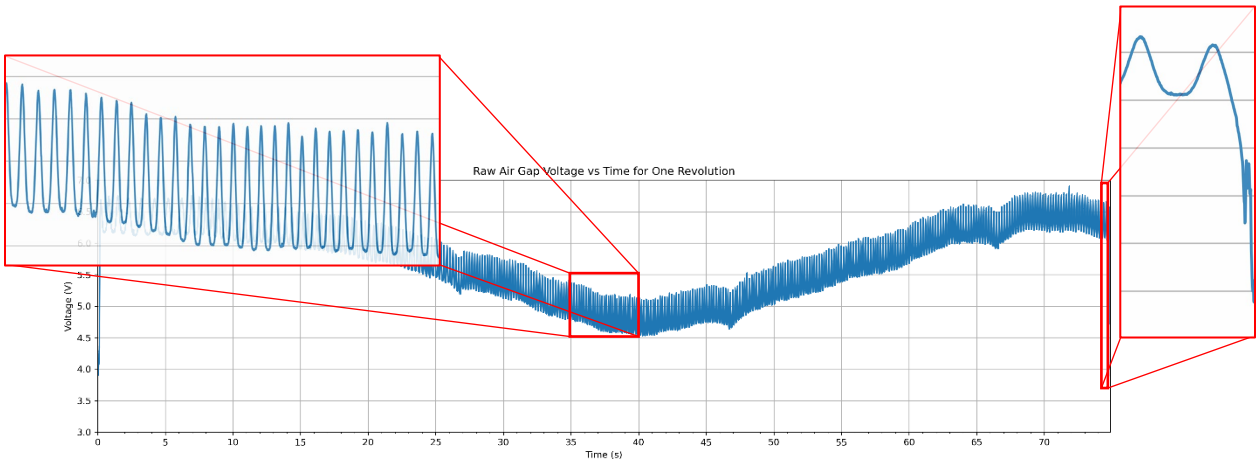


Figure 6 One revolution of air gap sensor voltage.

With the air gap probe and NFC antenna connected to the V and PD channels of the MPD 600 respectively, the overall prototypical system is shown in the block diagram in Figure 7. All the equipment mounted on the rotor must be battery powered. Because the air gap probe is an active sensor, a box was made with battery power, the sensor transducer, DC-to-DC voltage conversion, and appropriate sensor and data output connections. The MPD 600 was powered from the battery supplied when purchasing this device. The MCU 502 is powered from the laptop's universal serial bus (USB) port. All data is streamed into files on the data acquisition laptop. Monitoring and control of the data acquisition was carried out by the command-and-control laptop via a secure shell (SSH)

connection over a local wireless network. For tracking position, the OPR wire is mounted to a stator core packet and the packet location recorded for proper analysis. Any offset between the NFC antenna and air gap probe mounting locations must also be recorded for this purpose.

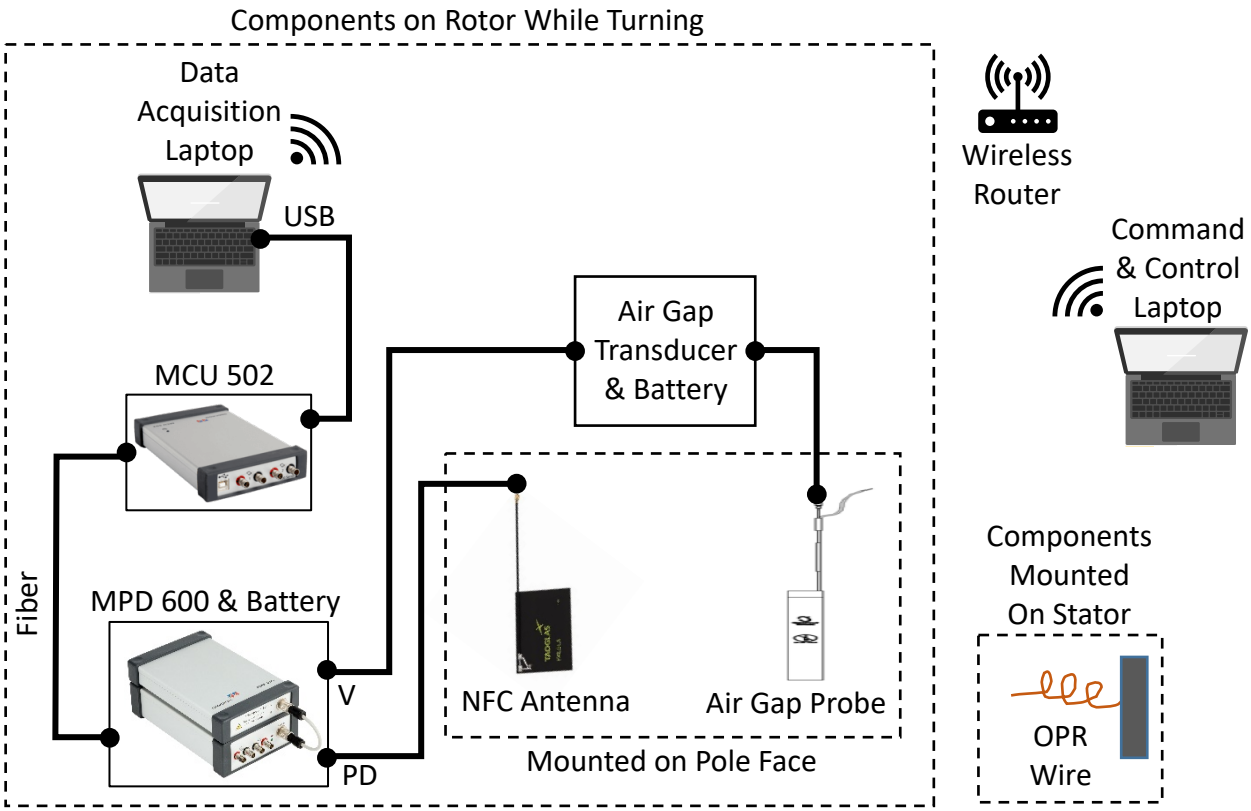


Figure 7 Block diagram of prototypical PD mapping system.

Operation of the prototypical system is carried out by operating the EMRT to slowly turn the rotor, typically around 0.5 to 1 revolution per minute, and initiating the data acquisition software from the command-and-control laptop. The data acquisition software interface was custom written for this research project and utilized the Omicron software's COM interface. Custom software is required because the Omicron software was designed to measure PD events as they appear relative to the phase of one power cycle (typically 50 or 60 Hz). Because one rotation of the rotor with the EMRT takes on the order of one minute to complete, a continuous stream of data for around one to two minutes was required from the PD measurement equipment. This relatively long, continuous stream (particularly of the voltage data) is not easily carried out within the Omicron software's graphical user interface. To obtain this continuous stream of data, two command line programs were written.

The first program, written in C# and called OmiCOMServer, acts as a server for the data stream from the Omicron MPD software. OmiCOMServer initializes the MPD system with critical values such as charge detection thresholds and calibration coefficients, instructs the hardware to monitor the voltage channel, and creates two named pipes for inter-process communication (IPC). There is one IPC pipe for PD data and another IPC pipe for voltage data. The voltage data pipe consists of a voltage value measured every 48 μs, as defined by the MPD hardware. No time data is transmitted with this voltage data, and the time spacing of voltage points is hardware defined. The PD pipe data is composed of a struct datatype for every detected PD event. Each struct contains the PD event's

charge, time of detection, and phase relative to the trigger. The charge value is in units of Coulomb, time of detection is in seconds from the time that the software was started. Phase is given as a value between 0 and 1, where 1 is a full period of the power cycle. However, because there is no correlation between the air gap voltage signal and the power cycle, the phase value is meaningless in this case. There are no incomplete structs sent through the pipe. Also, a fabricated PD event with a charge of 0 C is sent every 300 ms to transmit the data's time base if no PD events are measured.

The second program, written in C++ and called OmiCOMClientCPP, acts as the data consumer, and connects to the named IPC pipes created by the OmiCOMServer program. OmiCOMClientCPP allows the operator to start data recording on command. Data recording is performed by writing the data being transferred through each pipe into a corresponding plaintext file of comma separated values. Plaintext (rather than a relational database or similar) was chosen so that data could be tracked (and therefore backed up) in a human-readable way when using git version control. For the voltage pipe, OmiCOMClientCPP downsampled the data to every twentieth voltage value (or every 960 μs) to reduce throughput while writing data files. This was acceptable for the time scales observed in turning the rotor, and still allowed for recording a sufficient number of voltage samples per slot during even the fastest rotations. For the PD pipe, every struct was written to the corresponding plaintext file as one line of data. OmiCOMClientCPP can record up to 10 minutes of streamed data, barring any limitations of the underlying hardware the program is compiled on.

To perform a field test, the equipment is installed in a rotating machine. Both laptops are connected to the local wireless network. The command-and-control laptop connects to the data acquisition laptop over the network via SSH. Through the command-and-control laptop's SSH connection, the OmiCOMServer program is run on the data acquisition laptop to start and initialize the MPD interface. At this point, the test operator at the command-and-control laptop can start, stop, or check the status of the data pipes by entering the respective commands into the command prompt provided by OmiCOMServer. Once everything is initialized and running, the rotor is turned using the EMRT. Through the command-and-control laptop, recording of the PD and voltage data streams is initiated by running the OmiCOMClientCPP program. After visual confirmation that one revolution of data has been recorded (the air gap probe is visually verified to have passed the OPR signal wire at least twice, initial and final), the data recording is stopped by pressing the escape key. OmiCOMClientCPP monitors for the escape key, and, when detected, finishes reading from the data stream buffers and cleanly disposes of the pipe connections from memory. To extract meaningful information from the recorded data, post processing and analysis must be carried out as described in the next section.

## Prototypical System Field Testing and Results

Field testing was performed on Pump-Generator No. 1 (PG-1) at Mt. Elbert Powerplant. This asset was chosen because several years of traditional corona probe data were available, the asset was scheduled for a planned outage that aligned with the research schedule, and the powerplant's proximity to the TSC reduced travel (and therefore research) expenses. PG-1 is a 105.2 MVA, 11.5 kV rated pump-generator with a 330-slot winding with 10 parallel circuits per phase. Each parallel circuit contains eleven series-connected coils. The asset resides at an elevation of 9,600 feet above sea level, where cooling capabilities are reduced due to the lower air density. For this reason, the

stator winding has 13.8 kV class insulation and is de-ratted to an operating voltage of 11.5 kV. The stator coil throw covers 8 core teeth per coil. PG-1 was put in service in 1978, though didn't operate much until the early 1980s.

In contrast to traditional corona probe, unit preparation for this field testing was very simple. Other than the electrical and mechanical clearance (i.e., lock out tag out, which was already in place due to the planned outage) the only required disassembly was the removal of one deck plate and one air baffle. This minor disassembly allowed access to a rotor pole and the rotor-to-stator air gap. The OPR signal wire was mounted on a core packet between slots 255 and 256. This means that the next slot the air gap probe sensor encountered after detection of the OPR signal was 255 or 256 for counterclockwise (CCW) or clockwise (CW) rotation respectively. The NFC antenna and air gap probe were installed on the same pole face with a two-slot offset between them. This means the next slot the NFC antenna encountered after detection of the OPR signal was 253 or 254 for CCW or CW rotation respectively.

PD mapping was carried out by energizing one phase at a time to 6.6 kV (nominal line-to-ground voltage) at 60 Hz while turning the rotor with the EMRT. The two phases not energized with high-voltage were single-point grounded. The EMRT was connected to one of the grounded phases to control rotation. Additional safety-related components were added to the EMRT to protect the operator against the potential of an insulation failure resulting in accidental energization of the phase to which it was connected. Data recording for each test began and concluded slightly before and after the air gap probe contacted the OPR signal wire. During testing, contact was determined by visually watching rotor movement and viewing the area with the OPR signal wire. This allowed for the recorded data set for each PD mapping to contain more data than one full revolution, with the data between each OPR signal within the test run corresponding to exactly one revolution. Exactly one revolution of data could then be extracted later by identifying the OPR signal near the start and end of the data files. Four PD maps per phase were collected. Two were performed using CW rotation and two performed using CCW rotation, for a total of twelve PD maps under energized conditions. For each data collection, two files were generated, one for the voltage data and one for the PD data, each with the same unique time stamp appended to their filenames and corresponding to the time of test. These time stamps are how the individual data sets are identified, discussed, and compared during analysis.

Because of the different time bases between the PD and voltage data, significant data processing was required to produce visual representations of the PD maps. An API was written in the Python programming language to perform this data processing. The heart of this API is the Analyzer class, which runs many processing algorithms to format the data in a more efficient and usable form upon the initialization of an Analyzer object. The custom plotting methods and data structures of the initialized Analyzer object form the API, and the programmer can produce rich and detailed visual representations of the collected data with a method call in a single line of code. This API can be found on RISE, with the data, for others to utilize to reproduce the analysis here or otherwise investigate further[3].

The analysis schema beneath the API involves first identifying one revolution of voltage data. Then, correlation between the PD and voltage data time bases is performed, and one revolution of PD data is also extracted. The correlated data is stored in an efficient data structure, which the API can

[3] https://data.usbr.gov/

then access and visually present using custom plotting methods. To do all these tasks, an algorithm was written to identify the first and second detected OPR signals within the voltage data. The data between these signals corresponds to exactly one revolution of recorded voltage signal. The index (i.e., the point within the data array) at which these OPR signals occur within the full data record are then multiplied by 0.00096 s to obtain the time at which they occurred with respect to the start of the data recording. The factor of 0.00096 s is required because there is no time data within the voltage stream, though the down-sampled time between each voltage measurement is known to be this factor. Multiplying by this factor then converts from data position within the array to time within the data set. The PD time base is then referenced to the start of recording by subtracting the first recorded time within the set from all time values in this set. This re-referencing is required because the PD time base is referenced to the time at which the MPD software started rather than the start of recording. With the OPR signal times known, and PD referenced to the same time base, all PD events between the two OPR signal times then correspond to exactly one rotation of PD data.

With only one revolution of both voltage and PD data, the task is then to determine the time windows for each slot for which the NFC antenna was in front of that slot. All the PD events falling within each slot's time window is then attributed to that slot for the purposes of PD mapping. To do this, an algorithm was written to detect local maxima within one revolution of the voltage waveform as shown in Figure 8. The local maxima are detected slots within the stator winding and are represented by the red dots within Figure 8. Each red dot's horizontal position corresponds to an index multiplied by 0.00096 s to obtain the time at which the air gap probe was in front of that slot. The algorithm determines slot number from the number of maxima counted from the start of the rotation, which is referenced to the slot number encountered after the OPR signal, and depends on the direction of rotation.

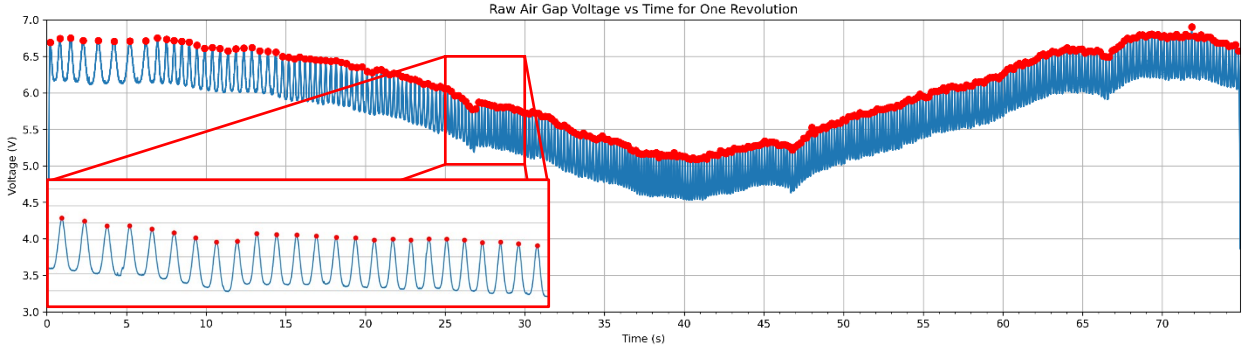


Figure 8 Plot showing algorithmic capability to locate each slot in time from the air gap sensor voltage.

Because the mounting locations of the air gap sensor and NFC antenna are offset by two slots for these tests, the algorithm accounts for this offset when calculating the time windows for each specific slot. The time windows are determined by bisecting the horizontal space between the local maxima (the red dots in Figure 8). The bisected time before and after the local maximum is the start and end of that slot's time window respectively. All PD events that were measured within a specific slot's time window are then associated with that slot number in the PD map.

Note that the method of referencing the PD time data to the start of the data acquisition, and then to the first OPR signal, relies on a PD event being detected very close to these reference points. In practice, this is not an issue, as PD data with one phase energized showed the average time between

detected PD events was around 1 ms. This means there is a very high probability of the first detected PD event falling within 1 ms of the actual recording start time. Because the referencing algorithm uses the time-of-detection for the first PD event measured, the accuracy of the new time base is likely on the order of 1 ms. However, if the PD threshold is set too high, and several seconds or more pass before measuring the first real PD event, the time reference will be based on the first fabricated PD event without charge. These PD events are produced by the MPD system specifically for timing reference and are spaced every 300 ms. If the timing happens to be such that the first one of these timing events is detected 300 ms into the data acquisition, the accuracy of the new PD time base would be 300 ms off. For this reason, it is advisable to ensure the PD threshold is set to ensure detection of thousands of PD events or more per second. However, it was found that if the PD threshold is set too low, the OmiCOMClientCPP program can drop data due to hardware limitations and data throughput. For these reasons, the ideal PD threshold was determined empirically, and remained 3 pC for all testing of energized phases.

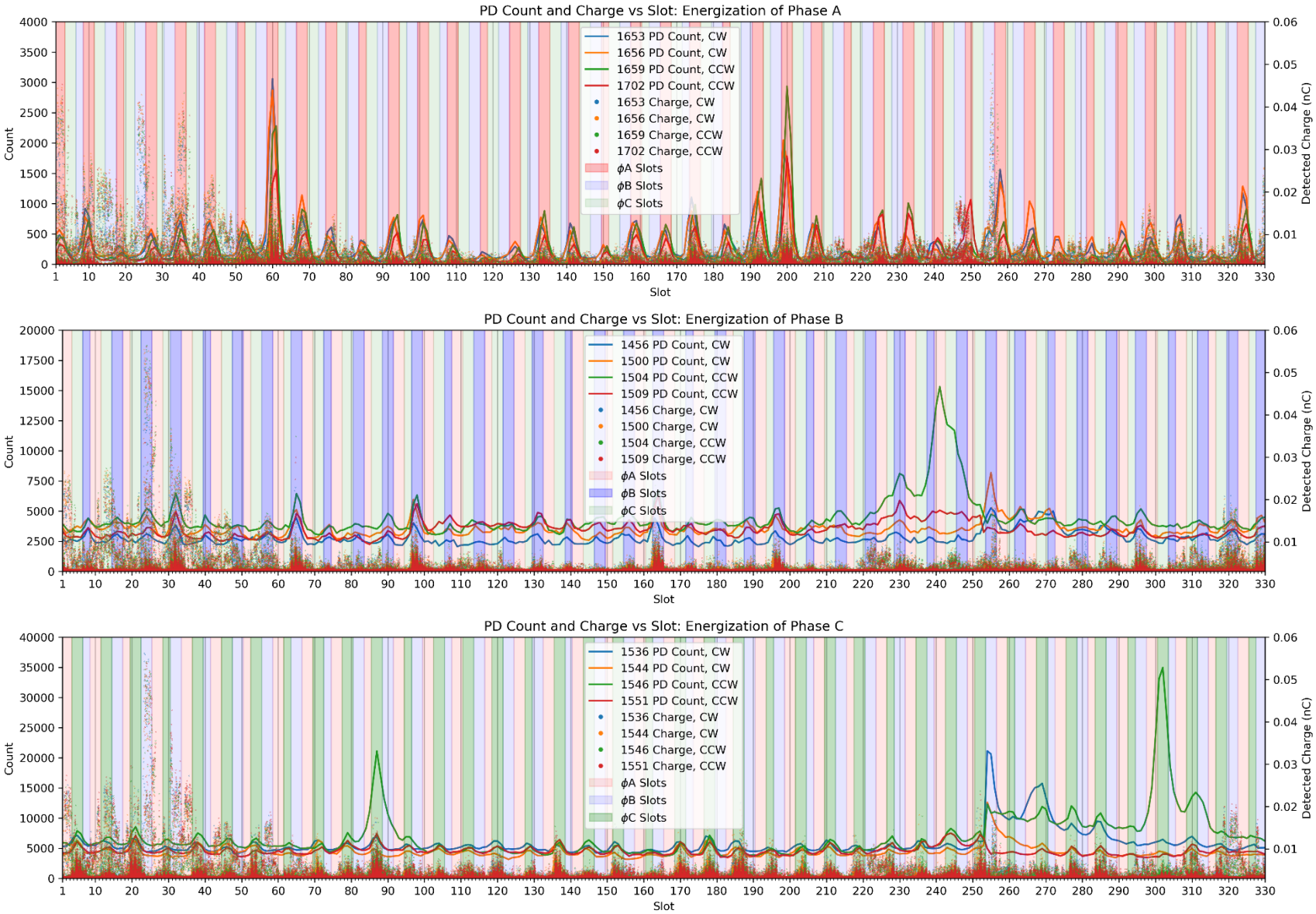


Figure 9 PD maps for each phase showing count and detected charge versus slot position for all tests.

Figure 9 shows the resulting PD maps for all tests of each energized phase. Each plot is titled with which phase was energized and shows both PD count and detected charge with respect to slot number for every test performed in that configuration. The legend shows the test run time stamp (as a test identifier) as well as the direction of rotation for that test. For all tests shown in Figure 9, the measurement band was 1.5 MHz and centered at 13.5 MHz. The PD charge threshold was set to 0.003 nC. Because there is no known reliable means of calibrating detected charge to actual charge, a divider factor of 1.0 was used for all tests. This means the actual charge transferred in any given PD event is likely much larger than presented here. The background coloring in each plot highlights coil groups and shows the slots with a top bar corresponding to phases A, B, and C highlighted in red, blue, and green respectively. When looking at these plots, there is clearly visual correlation between PD activity and slots with top bars associated with the energized phase. Moreover, there appears to be slot level resolution in the detected charge patterns within coil groups of the energized phase.

An interesting phenomenon was discovered when an attempt was made to map the stator winding with an IEC standard PD calibration signal connected to the line-end of phase A (not energizing any phases with high-voltage). Specifically, an interesting pattern was discovered at the slot location where the OPR signal would be encountered on the voltage channel. The PD maps that led to this discovery are shown in Figure 10 between slots 253 and 254 (the slots the NFC antenna is in front of just after the OPR signal is detected depending on direction of rotation).

In this plot, just after the OPR signal is detected, there is elevated PD count detected by the NFC antenna. Because the OPR signal produces a large, fast change in voltage on the V channel of the MPD system, this signal necessarily contains high frequency content. It is therefore hypothesized that the increased PD count near the OPR signal is due to poor channel isolation between the PD and V channels on the MPD 600. In other words, voltage on the PD channel is induced due to coupling of high frequencies from the V channel. It is unknown whether the increased PD count around slot 254 in the phase C tests shown in Figure 9 are due to the same phenomenon, but such a hypothesis should not be ruled out without further investigation.

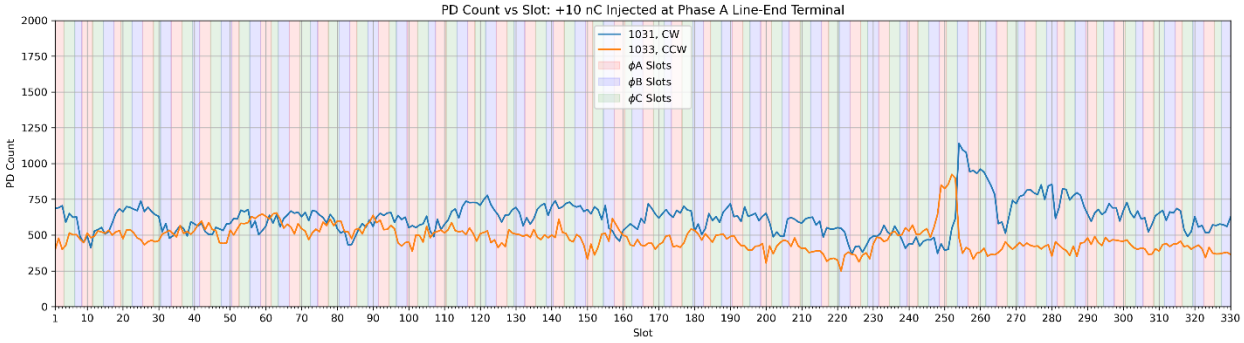


Figure 10 PD map showing interesting pattern near OPR signal location.

Traditional corona probe data was also available for this stator winding. These historical tests can be seen in Figure 11 for years 1999, 2004, 2009, and 2014. Unfortunately, while the corona probe data shows visual similarities to the NFC data, a direct comparison of the data sets cannot be made. For the historical corona probe tests:

- From 2004 to 2009, only one phase was energized at a time and only the slots containing top bars of the energized phase were measured. In addition, slots that did not exhibit high readings during the last historical test were not measured.
- In 1999, while all slots were measured, they were measured with all phases energized at the same time, which limits phase-to-phase PD activity.
- Moreover, because the traditional corona probe has a different pass band than the NFC antenna, it is not clear whether they would even detect the same PD events. However, if the single-phase energization measurements were taken at every slot, a cross-correlation could have been performed between the NFC data and traditional corona probe data.

Such quantitative comparisons would be part of the goal of potential future research.

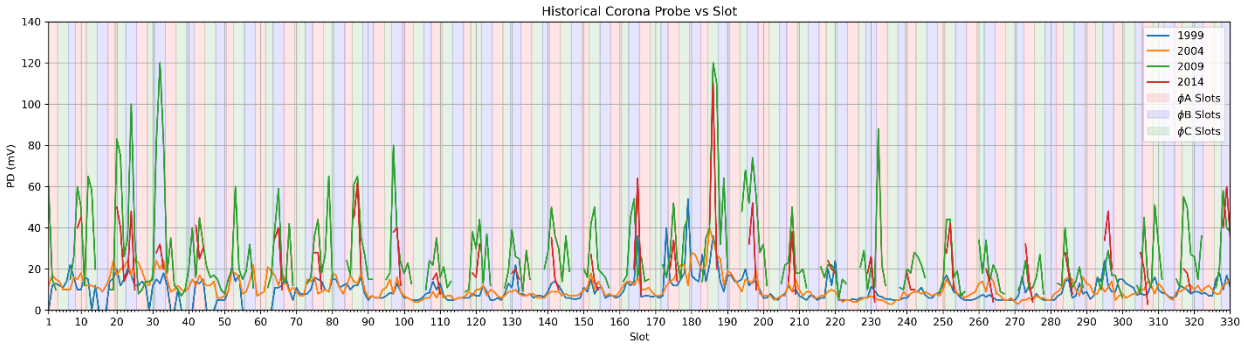


Figure 11 Historical corona probe data.

# Conclusions

The results of this and previous research clearly show that presently commercially available products can be adapted to detect and map PD within large diameter machines using NFC antennas.

Trending of such PD mapping could prove very valuable to asset managers and stakeholders. The problem with galvanically decoupling PD signals from windings during online monitoring is a problem of detecting PD signals located physically far from the decoupling location, which results in low resolution for the asset as a whole. The traditional methods either require assumptions that the rest of the winding is aging like the few bars or coils that are close to the couplers; or it requires significant cost, hazard, and risk to gain slot-by-slot PD resolution by performing a corona probe test. This method of PD mapping with NFC antennas and commercially available components has the potential to solve both the resolution and cost issues. Further, this method is widely applicable to large diameter machines across the industry meaning the impact on improving high-voltage insulation diagnostics of rotating machines is high.

More research is required to further advance this method of PD mapping. This research showed different band passes of different sensing technology measures different PD events. More investigation is needed to determine whether this higher frequency PD is of any consequence to increased insulation degradation over time, or whether NFC detected PD events correlate with higher energy, lower-frequency events like surface discharge. The testing included herein only

utilized one NFC antenna, mounted at the same axial location in the machine for each test. Future advances should include several NFC antennas axially spaced along a rotor pole face. Due to the hypothesized crosstalk between the V and PD channels when the OPR signal is encountered, a better method for detecting the location of one revolution needs to be pursued. Insights from Omicron would be welcomed to better understand the hardware within the MPD 600 or 800, and whether there is significant jitter between time bases within the hardware. Further investigation into whether phase data can be incorporated into this PD mapping process is also needed, perhaps obtaining phase resolved PD profiles for each slot mapped. This study also found no clear means of calibrating detected charge to obtain actual charge. Detected charge attenuation scales with the distance between the NFC antenna and source, however, more dependencies may be present, and further insight on this topic is needed.

Funding has been sought to further advance the prototypical system presented here. Due to the complexities and costs associated with asset outages, it is difficult to find test specimens for this research. This means that this research needs to align with routine work performed during routine outages. If this system is made more robust and easier to use, it could be brought to the field and used much more frequently. More frequent use would allow for further investigations into more advanced PD mapping, which would ultimately improve industry understanding of a very complex system.

# References

Lapenna, J., E. Eastment. 2018. Power System Diagnostics: Partial Discharge Attenuation in Large-Diameter Salient-Pole Machines. Bureau of Reclamation Research and Development Office, Science and Technology Program, Final Report ST-2018-1776-01.

Lapenna, J. 2017. Feasibility of Corona Mapping and Partial Discharge Detection in Stator Windings Using Patch Antennas. Bureau of Reclamation Research and Development Office, Science and Technology Program, Final Report ST-2017-1711-01.

Texas Instruments, 2021. THS4303 Wideband Fixed-Gain Amplifier Datasheet. https://www.ti.com/product/THS4303. Date Accessed 08/30/2021.

International Electrotechnical Commission (IEC), 2021. IEC 60270:2000 High-Voltage Test Techniques – Partial Discharge Measurements. https://webstore.iec.ch/publication/23841. Date Accessed 08/30/2021.

Iris Power, 2021. Stator Slot Couplers (SSC) – Partial Discharge Monitoring. https://irispower.com/products/stator-slot-couplers-ssc/. Date Accessed 08/30/2021.

Lapenna, J. 2021. Development and Refinement of Rotor Turning Device for Safer and More Efficient Maintenance and Diagnostic Tasks. https://www.usbr.gov/research/projects/detail.cfm?id=21006. Date Accessed 08/30/2021.

Baker Hughes, 2021. 4000 Series Air Gap Sensor System Datasheet – 167885. https://www.bakerhughesds.com/bently-nevada/sensors/hydro-sensors. Data Accessed 08/30/2021.

# Glossary

**Partial Discharge (PD).** Localized electrical discharges in insulating material only partially bridging the insulation between the conductors creating the electric potential. In practice, this is usually due to small voids and imperfections within the insulating material. Generally, when the electric field across these voids and imperfections increases above the ionization energy of the material or gas within the void, breakdown occurs, and charge is transferred across the localized point. Over time, the ionization, resultant heat, and chemical byproducts can further expand the area of localization and degrade the insulation from the inside out. This charge transfer across the localization is a high-frequency, wide-band current impulse, which can be measured by specialized equipment.

**Near Field Communication (NFC).** Near field communication is a set of communication protocols for two electronic devices to communicate over short distances (on the order of 1 inch) based on radio frequency identification (RFID) standards. The standard operates on the open and unlicensed Industrial, Scientific, and Medical (ISM) radio band of 13.56 MHz $\pm$ 7 kHz, though, in practice, the bandwidth can be over 1 MHz wide to increase data rates. Because the communication distances are much smaller than the wavelength within this band, the transmitter/receiver interaction is described as near field. This near-field interaction is through the alternating magnetic field (flux) through the antenna(s). Because the antennas are much smaller than the band's wavelength, they have very little susceptibility to interference from radiated electric fields (i.e., noise) within their receiving spectrum. In the context of this project, no aspects of the actual communication protocols were implemented. However, due to the operating principles of near-field antennas, they have shown to be good candidates for PD measurement across a small air gap.

**Application Programming Interface (API).** An application programming interface is interconnected software which creates an interface for more simplistic programs to utilize when interacting with a more complex system. In the context of this project, the API simplifies the data analysis so that an interested programmer can use the data for their own purposes without having to code the algorithms for peak detection and synching of time bases from scratch. The programmer need only interact with the custom functions, methods, and data structures of the API.

**Component Object Model (COM).** The component object model is an agreed upon standard for creating binary software components that can interact. COM is a platform independent, distributed, object-oriented system. In the context of this project, data from one running process are piped to another custom process which write these data to plaintext files for later analysis. This interaction between the custom processes used to record the data and the process communicating with the measurement hardware is facilitated through COM interfaces. Without COM, communication between these processes would be much more difficult to implement, and would likely have required significant reverse engineering of the measurement hardware's binary (beyond the scope of this project).

**Git Version Control.** Git is open-source software for tracking changes to a set of files of any type. Git allows reverting selected files or the entire set back to any previously recorded state, compare changes over time, and merge new changes into the file set in a controlled manner.

While git can keep track of changes to any type of file, changes are much more easily compared in a human-readable way when working with plaintext files.